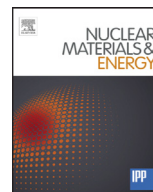




Contents lists available at ScienceDirect

## Nuclear Materials and Energy

journal homepage: [www.elsevier.com/locate/nme](http://www.elsevier.com/locate/nme)

## Comparative small angle neutron scattering (SANS) study of Eurofer97 steel neutron irradiated in mixed (HFR) and fast spectra (BOR60) reactors

R. Coppola<sup>a,\*</sup>, E. Gaganidze<sup>b</sup>, M. Klimenkov<sup>b</sup>, C. Dethloff<sup>b</sup>, R. Lindau<sup>b</sup>, M. Valli<sup>c</sup>, J. Aktaa<sup>b</sup>, A. Möslang<sup>b</sup>

<sup>a</sup> ENEA-Casaccia, Via Anguillarese 301, 00123 Roma, Italy

<sup>b</sup> KIT-IAM, P.O. Box 3640, D-76021 Karlsruhe, Germany

<sup>c</sup> ENEA- Faenza, Via Ravennana 186, 48018 Faenza, RA, Italy

## ARTICLE INFO

## Article history:

Received 16 November 2015

Revised 2 February 2016

Accepted 23 February 2016

Available online xxx

## Keywords:

Neutron irradiation

Ferritic/martensitic steels

Small-angle neutron scattering

Electron microscopy

## ABSTRACT

This contribution presents a comparative microstructural investigation, carried out by Small-Angle Neutron Scattering (SANS), of ferritic/martensitic steel Eurofer97 (0.12 C, 9 Cr, 0.2 V, 1.08 W wt%) neutron irradiated at two different neutron sources, the HFR-Petten (SPICE experiment) and the BOR60 reactor (ARBOR experiment). The investigated “SPICE” sample had been irradiated to 16 dpa at 250 °C, the investigated “ARBOR” one had been irradiated to 32 dpa at 330 °C. The SANS measurements were carried out under a 1 T magnetic field to separate nuclear and magnetic SANS components; a reference, un-irradiated Eurofer sample was also measured to evaluate as accurately as possible the genuine effect of the irradiation on the microstructure. The detected increase in the respective SANS cross-sections of these two samples under irradiation is attributed primarily to the presence of micro-voids, for neutron contrast reasons; it is quite similar in the two samples, despite the higher irradiation dose and temperature of the “ARBOR” sample with respect to the “SPICE” one. This is tentatively correlated with the higher helium content produced under HFR irradiation, playing an important role to stabilize the micro-voids under irradiation. In fact, the size distributions obtained by transformation of the SANS data yield a micro-void volume fraction of 1.3% for the “SPICE” sample and of 0.6% for the “ARBOR” one.

© 2016 The Authors. Published by Elsevier Ltd.

This is an open access article under the CC BY license (<http://creativecommons.org/licenses/by/4.0/>).

### 1. Introduction

The behavior of Eurofer97 steel (0.12 C, 9 Cr, 0.2 V, 1.08 W wt%) under neutron irradiation has been extensively investigated, both by post-irradiation mechanical testing and by microstructural examinations, in a variety of irradiation conditions to predict as accurately as possible its performance in service; in fact this steel is the European reference for fusion applications. More specifically, it has been neutron irradiated at two different neutron sources, the High Flux Reactor (HFR) – Petten (“SPICE” irradiation experiment, ref. [1,2]) and the BOR60 Reactor (“ARBOR” irradiation experiment, ref. [3,4]). These two experiments were designed to investigate changes in Eurofer mechanical properties and microstructure under neutron irradiation, at  $T \leq 450$  °C to a volume average dose of 16.3 dpa in the case of SPICE and at 330 °C up to 70 dpa in the case of ARBOR.

Post-irradiation microstructural characterization has been carried out by transmission electron microscopy (TEM) [5–8] for ARBOR samples; TEM and small-angle neutron scattering (SANS) results on SPICE samples have also been published [9–13]. In this paper SANS results are compared, obtained on one ARBOR and one SPICE sample, already characterized by other techniques, in order to contribute in understanding the microstructural effects produced in Eurofer97 steel at different neutron sources. In general, quantitative comparisons between samples of a same steel irradiated by different neutron irradiation experiments (not necessarily at different neutron sources) are not straightforward, mostly because it is not possible to perfectly monitor and reproduce parameters such as the irradiation temperature, for instance, and consequent effects on the material. Additionally, in the present case the two investigated samples, available at the time when the SANS experiments had been scheduled, differ not only in irradiation temperature but much more in nominal irradiation dose. Therefore, the experimental results and suggested interpretation presented in this paper are not intended as conclusive ones but as a first step to contribute

\* Corresponding author. Tel.: +39 0630484724.

E-mail address: [roberto.coppola@enea.it](mailto:roberto.coppola@enea.it) (R. Coppola).

<http://dx.doi.org/10.1016/j.nme.2016.02.008>

2352-1791/© 2016 The Authors. Published by Elsevier Ltd. This is an open access article under the CC BY license (<http://creativecommons.org/licenses/by/4.0/>).

in understanding this complex matter, to be hopefully soon completed by further investigations of ARBOR and SPICE samples, irradiated to a same nominal dose level.

## 2. Material characterization

The following Eurofer97 samples were investigated by SANS:

Un-irradiated reference Eurofer 97-1 Heat E 83697 (980 °C 0.5 h/air + 760 °C 1.5 h/air)

“SPICE” Eurofer 97-1 E 83697 (YW01) 16.3 dpa 250 °C (1040 °C/0.5 h + 760 °C/1.5 h)

“ARBOR” Eurofer 97-1 E 83697 (E102K) 31.8 dpa 332 °C (980 °C/0.5 h + 760 °C/1.5 h).

The un-irradiated reference was machined as a platelet  $1 \times 1 \times 0.1 \text{ cm}^3$ . The two irradiated samples were obtained by cutting, in the hot cells, from each of the corresponding KLST samples a slice  $0.8 \times 0.4 \times 0.1 \text{ cm}^3$ ; they were subsequently mounted each one on a Cd shielded sample-holder to allow safe transportation to the neutron source and manipulation during the SANS experiment (activity level  $4.42 \times 10^{10} \text{ Bq}$ , contact dose rate in an Al capsule 14 mSv/h).

TEM characterization of precipitates in un-irradiated Eurofer97 can be found in ref. [14]. Post-irradiation characterization relating to the SPICE experiment is reported in ref. [1]. TEM studies of SPICE samples are still underway, TEM results on HFR irradiated Eurofer97 up to 8.3 dose level (“SUMO” experiment), focusing mainly on the characterization of dislocation loops and Burgers vectors orientation, are reported in ref. [13]. Concerning the ARBOR material, ref. [5] provides an assessment of neutron irradiation effects in Eurofer97. Ref. [5] also presents the results of TEM observations on ARBOR samples, showing that the volume density of the observed micro-voids and dislocation loops increases of almost one order of magnitude between 15 dpa and 32 dpa irradiation dose. New TEM results on these samples are presented at this conference [7] and shown in Fig. 1; they indicate a much smaller density of micro-voids compared to SPICE.

## 3. Experimental technique

General information on the SANS technique can be found in refs. [15,16] and in previous works on fusion steels [9–12]. Defining the modulus of the scattering vector  $Q = 4\pi \sin\theta/\lambda$  (where  $2\theta$  is the full scattering angle and  $\lambda$  the neutron wavelength), in the case of magnetic samples the total SANS cross-section  $d\Sigma(Q)/d\Omega$

(where  $\Omega$  stands for the solid angle) can be written as the sum of two terms, a nuclear and a magnetic one

$$d\Sigma(Q)/d\Omega = d\Sigma(Q)/d\Omega_{nucl} + d\Sigma(Q)/d\Omega_{mag}\sin^2\alpha \quad (1)$$

where  $\alpha$  is the azimuthal angle on the detector plane. Applying an external magnetic field to saturate the sample magnetization in the sample, the ratio  $R(Q)$  of the SANS components perpendicular and parallel to this field

$$R(Q) = \frac{d\Sigma(Q)/d\Omega_{nucl} + d\Sigma(Q)/d\Omega_{mag}}{d\Sigma(Q)/d\Omega_{nucl}} = 1 + (\Delta\rho)_{mag}^2/(\Delta\rho)_{nucl}^2 \quad (2)$$

is related to the composition of the microstructural inhomogeneities and its dependence on  $Q$  implies that defects of different size or composition are present in the investigated sample,  $(\Delta\rho)^2$  being the “contrast” or square difference in neutron scattering length density (nuclear and magnetic respectively) between the observed nuclear and magnetic inhomogeneities and the matrix [15,16]. In the case of Eurofer97, assuming that the carbide precipitate composition is  $\text{Cr}_{14}\text{Fe}_8\text{W}_{0.7}\text{V}_{0.3}\text{C}_6$  [14] a contrast value of  $2.13 \cdot 10^{20} \text{ cm}^{-4}$  is found, while for the case of micro-voids the contrast is equal to the scattering length density of Eurofer97 itself, that is  $5.51 \cdot 10^{21} \text{ cm}^{-4}$ , more than one order of magnitude larger.

Assuming that the investigated material is a diluted system of inhomogeneities, the SANS nuclear and magnetic cross-sections can each one be written as

$$d\Sigma(Q)/d\Omega = (\Delta\rho)^2 \int_0^\infty dR N(R) V^2(R) |F(Q, R)|^2 \quad (3)$$

where  $N(R)dR$  is the number per unit volume of defects with a size between  $R$  and  $R+dR$ ,  $V$  their volume and  $|F(Q, R)|^2$  their form factor (assumed spherical in this case) and  $(\Delta\rho)^2$  is the nuclear or magnetic “contrast”. The volume distribution function is defined as:

$$D(R) = N(R)R^3 \quad (4)$$

$N(R)$  was determined, by transformation of Eq. (3), using the method described in [17] and more recently discussed in [18–20]. This code assumes that the size distribution function can be described by a set of cubic B-spline functions, with equispaced knots in log  $R$  scale (to account for the simultaneous presence of defects sizes differing in order of magnitude) and the constraint that the distribution is positive or null. The number of splines is determined by the  $R$ -range where the size distribution is to be explored

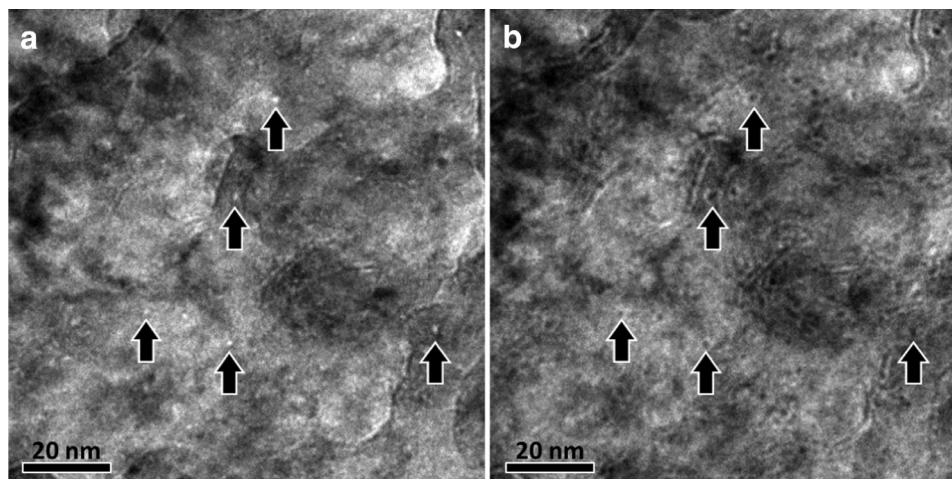
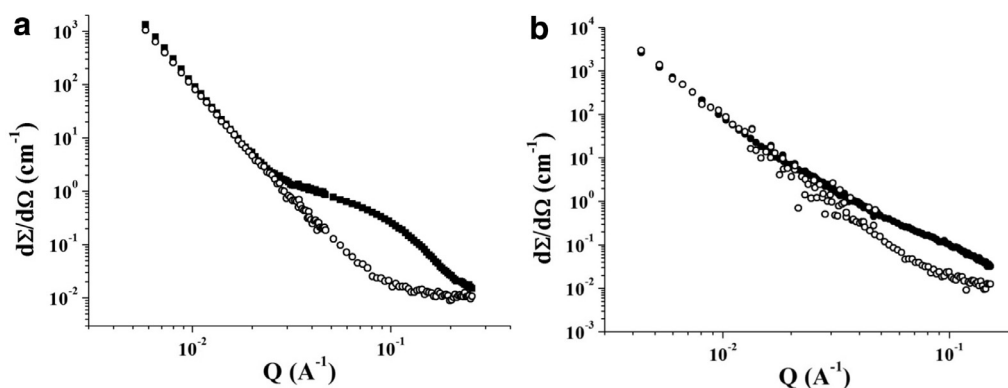
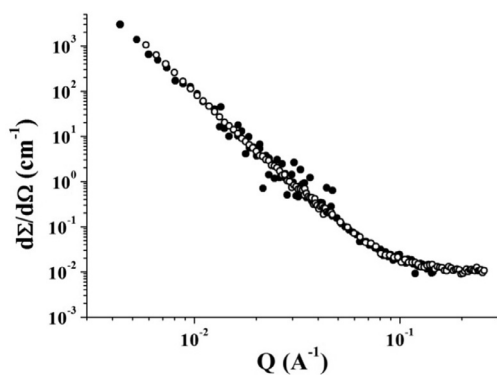


Fig. 1. TEM micrograph for Eurofer97/1 irradiated at 332 °C to 32 dpa (“ARBOR”) in a) underfocus (–500 nm) and b) overfocus (+500 nm) condition. Some voids are marked by arrows [7].



**Fig. 2.** Nuclear SANS cross-sections for the Eurofer97/1 un-irradiated reference (empty circles both in 1a and in 1b), for Eurofer97/1 irradiated at 250 °C to 16.3 dpa (“SPICE”, full circles in 1a) and for Eurofer97/1 irradiated at 332 °C to 31 dpa (“ARBOR”, full circles in 1b).



**Fig. 3.** Nuclear SANS cross-sections for the Eurofer97/1 un-irradiated reference measured in the two different SANS experiments reported in Section 3 (empty circles “SPICE” SANS experiment, full circles “ARBOR” SANS experiment).

(always larger than the range where different sizes can be effectively resolved) and by the required degree of detail.

The SANS measurements were carried out at the D22 instrument at the High Flux Reactor of the Institut Max von Laue-Paul Langevin ILL, Grenoble. Due to their high activity, the two irradiated samples had to be transported to the neutron source in different times and included in two separate SANS experiments. In the case of the SPICE sample a neutron wavelength of 6 Å and sample-to-detector distances of 2 m and 11 m were selected in order to cover a  $Q$ -interval ranging from  $3 \times 10^{-3}$  to  $0.26 \times 10^{-1} \text{ \AA}^{-1}$ , corresponding to sizes  $2R \sim \pi/Q$  varying between 10 and 1000 Å approximately. In the case of the ARBOR sample-to-detector distances of 3.5 m and 11.2 m with a neutron wavelength  $\lambda$  of 6 Å were utilized ( $Q$  interval ranging from  $2 \times 10^{-3}$  to  $0.16 \text{ \AA}^{-1}$ , which corresponds to particle sizes ranging from 20 to 1500 Å approximately); for technical reasons, shorter counting times had to be selected during this experiment. In both experiments, an external 1 T magnetic field was applied, the same reference, un-irradiated Eurofer97 sample was measured and calibration to absolute SANS cross-section was obtained by the ILL standard programs. The statistically evaluated experimental errors on the data reported in Figs. 2–5 are generally below 3%.

#### 4. Results and discussion

Fig. 2a and b show the nuclear SANS cross-section measured for the SPICE and for the ARBOR sample respectively, together the nuclear component of the reference sample; Fig. 3 shows the comparison of the nuclear SANS cross-sections measured for the reference sample in the two SANS experiments. The  $R(Q)$  ratio mea-

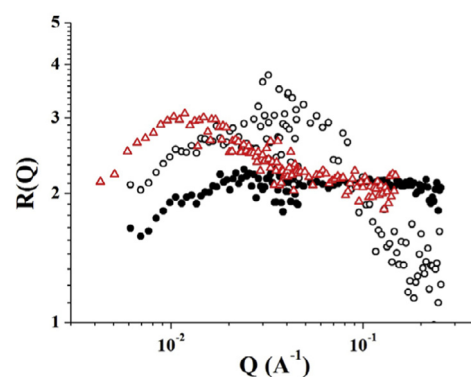


**Fig. 4.**  $R(Q)$  ratio for the Eurofer97/1 un-irradiated reference (empty circles, “SPICE” SANS experiment), for Eurofer97/1 irradiated at 250 °C to 16.3 dpa (“SPICE”, full circles) and for Eurofer97/1 irradiated at 332 °C to 31 dpa (“ARBOR”, triangles).

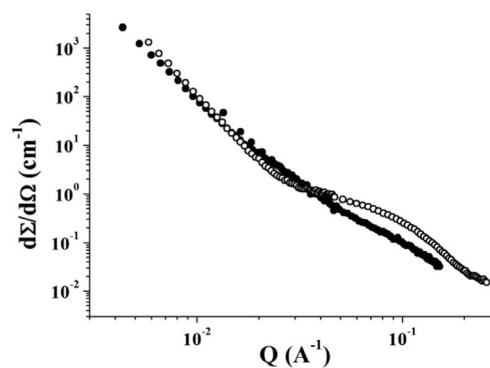


**Fig. 5.** Nuclear SANS cross-section for Eurofer97/1 irradiated at 250 °C to 16.3 dpa (“SPICE”, empty circles) and for Eurofer97/1 irradiated at 332 °C to 31 dpa (“ARBOR”, full circles).

asured for the three investigated samples is shown in Fig. 4. The nuclear SANS components of the SPICE and of the ARBOR Eurofer97 irradiated samples are directly compared in Fig. 5. At first, Fig. 3 shows that the SANS data obtained in the two different SANS experiments are perfectly comparable, despite the lower statistics for the one in which the measurement of the ARBOR sample was included.

Commenting the irradiation effect in the SPICE sample (Fig. 2a), it has to be noted that preliminary SANS results on this same sample were reported in ref. [11], referring to a previous SANS experiment. However, as mentioned in that paper, a reliable exploitation of those results was not possible because of uncertainties in the

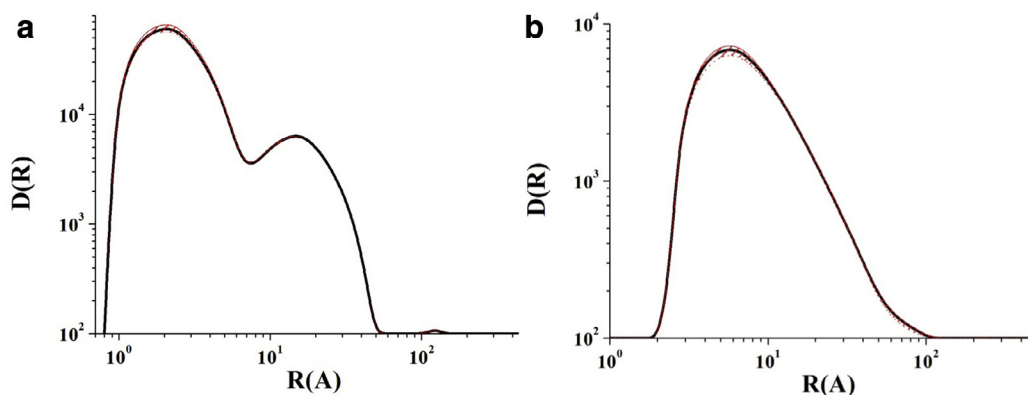


**Fig. 6.** Volume distribution functions  $D(R)$ , in  $\text{\AA}^{-1}$ , attributed to the presence of micro-voids in Eurofer97/1 irradiated at 250 °C to 16.3 dpa (“SPICE”, a) and for Eurofer97/1 irradiated at 332 °C to 31 dpa (“ARBOR”, b); the dashed area represents the 80% confidence band [18,19].

available, un-irradiated reference: in fact, that sample had most probably not undergone the same thermal treatment as the Eurofer97 sample utilized for this new experiment (Section 2). Fig. 2a shows that in the SPICE sample the changes in the SANS cross-section under the effect of the irradiation are concentrated in a  $Q$ -region corresponding to defect sizes ranging between 10 and 50  $\text{\AA}$ ; for smaller  $Q$ -values ( $<0.4 \text{\AA}^{-1}$ ) corresponding to much larger sizes, no difference is detected between reference and irradiated sample, both showing a  $Q^{-4}$  “Porod” behavior [15,16], to be possibly attributed to precipitates as large as 500–700  $\text{\AA}$  [19,20]. In the case of the ARBOR sample, Fig. 2b shows that the effect of the irradiation is not restricted to such a concentrated size region as for the SPICE sample but is quite modest; this is better shown in Fig. 5, comparing the two irradiated samples directly. Additional, useful information is provided by the  $R(Q)$  ratio in Fig. 4. For the un-irradiated, reference Eurofer97 sample it is strongly dependent on  $Q$ , which implies the presence of different kinds of defects, and reaches values around 3, compatible with carbide precipitates [18,19]. For the SPICE sample it is nearly constant over a wide  $Q$  range and nearly equal to 2, in agreement with previous results on SPICE samples irradiated to lower dose levels [10] and with the interpretation that the SANS effect is in this case mostly due to micro-voids, which behave as magnetic holes in the fully magnetized Eurofer97 matrix. For the ARBOR sample,  $R(Q)$  is also nearly equal to 2 down to  $Q$  corresponding to a size of 100  $\text{\AA}$ , then increases significantly: this can be correlated with the TEM results of ref. [5], showing that, in this size range, both micro-voids and larger dislocation loops / clusters are present in this same ARBOR material.

The defect size distribution for the two irradiated samples have been determined transforming the SANS cross-sections shown in Fig. 5; in the case of the SPICE sample, the region for  $Q < 0.4 \times 10^{-1} \text{\AA}^{-1}$  was not considered because here the difference between the SANS cross-sections of reference and irradiated sample is smaller than the experimental errors (Fig. 2a). Fig. 6a and b shows the distributions determined assuming, in a first approximation, that the SANS effect is originated by micro-voids in both samples: this could not be entirely appropriate for the ARBOR sample, nevertheless, as explained in Section 3, a strong contribution from micro-voids has to be anyhow expected due to the high value of their neutron contrast. Under this simplified assumption, the SPICE sample presents a higher and broader distribution with respect to the ARBOR one, with corresponding micro-void volume fractions of 1.3% for the SPICE sample (in good agreement with the values reported in [10]) and of 0.6% for the ARBOR one. Additional metallurgical information on the chemical composition of the defect clusters observed in the ARBOR sample would in principle allow to transform its SANS cross-section by introducing a second contrast

value to try and model the presence of this second type of defects (Fig. 4). However, the SANS cross-sections shown in Fig. 5 clearly suggest that the effect of the irradiation on micro-void growth in the same material seems not to increase with the nominal dose level.

## 5. Conclusions

One SPICE and one ARBOR Eurofer97/1 samples, irradiated at two different temperatures and dose levels, have been investigated by SANS to contribute in understanding the microstructural effects associated to mixed and fast spectrum reactor irradiations. The results on the SPICE sample are consistent with those found for lower dose level [10,11] under mixed spectrum, assuming that in this case the SANS effect is mostly due to micro-voids, and will be the object of a new scientific publication on dose effects in Eurofer97/1 between 2.8 and 16 dpa. The results on the ARBOR sample are qualitatively consistent with available TEM observation on this material (ref. [5] in particular) but predict a micro-void volume fraction lower than the one detected, for half dose value, in the SPICE sample. This is tentatively attributed to the fact that there is nearly no helium production in BOR 60 whereas  $\sim 10$  appm He is produced after HFR irradiation of Eurofer97: though 10 appm is not large, it can play a significant role in stabilizing the micro-voids during irradiation. Additionally this is also consistent with a significant SANS contribution of defect clusters (much smaller neutron contrast) in the ARBOR sample as well as by the different volumes sampled by SANS and TEM, which reflect in statistics differing for orders of magnitude. It is however clear that the SANS measurement of the ARBOR sample irradiated to 15 dpa dose will be indispensable to clarify these results. It should be checked whether they can be correlated with the higher helium production associated to the mixed spectrum irradiation, which might result in a considerably lower micro-void concentration in the “ARBOR” sample with respect to the “SPICE” one. Finally, the fact that the consistently higher dose level of the ARBOR sample does not reflect in a corresponding increase of the SANS effect compared to the SPICE sample, might also suggest a good resistance of Eurofer97 to micro-void nucleation.

## Acknowledgments

This work, supported by the European Commission under the contract of Associations, was carried out within the framework of the European Fusion Development Agreement. The views and opinions expressed herein do not necessarily reflect those of the European Commission.



## References

- [1] E. Gaganidze, H.-C. Schneider, B. Dafferner, J. Aktaa, *JNM* 355 (2006) 83–88.
- [2] E. Materna-Morris, A. Möslang, H.-C. Schneider, *JNM* 442 (2013) S62–S66.
- [3] C. Petersen, Karlsruhe Institut für Technologie, FZKA 7517, 2010, 1–16.
- [4] E. Gaganidze, C. Petersen, *KIT Sci. Rep.* 7596 (2011) 1–12.
- [5] O. Weiss, E. Gaganidze, J. Aktaa, *J. Nucl. Mater.* 426 (2012) 52–58.
- [6] C. Dethloff, et al., *J. Nucl. Mater.* 454 (2014) 112–118.
- [7] C. Dethloff, E. Gaganidze, *ICFRM17 Proceedings*.
- [8] S. Rogozhkin, et al., *Inorganic Materials: Applied Research*, 4, Pleiades Publ. Ltd, 2013, pp. 112–118.
- [9] R. Coppola, R. Lindau, M. Magnani, R.P. May, A. Möslang, J.W. Rensman, B. van der Schaaf, M. Valli, *Fusion Eng. Des.* 75–79 (2005) 985–988.
- [10] R. Coppola, R. Lindau, R.P. May, A. Möslang, M. Valli, *J. Nucl. Mater.* 386–388 (2009) 195–198.
- [11] R. Coppola, M. Klimenkov, R. Lindau, A. Möslang, M. Valli, A. Wiedenmann, *J. Nucl. Mater.* 409 (2011) 100–105.
- [12] R. Coppola, M. Valli, EFDA Report for MAT-IREMEV—Task Agreement, 2013, Task WP13\_MAT\_01\_IREMEV\_05\_02/ENEA\_Frascati/PS, Dec. 2013.
- [13] M. Klimenkov, et al., in: Poster Presentation at ICFRM16 Conference, Beijing, 2013.
- [14] M. Klimenkov, R. Lindau, E. Materna-Morris, A. Möslang, *Prog. Nucl. Eng.* 57 (2013) 8–13.
- [15] G. Kostorz, R.W. Cahn, P. Haasen, *Physical Metallurgy*, North Holland, 1983, pp. 793–853.
- [16] M.T. Hutchings, C.G. Windsor, K. Sköld, D.L. Price, *Methods of Experimental Physics*, vol. 23–c, Neutron Scattering, Academic, 1987, pp. 405–482.
- [17] M. Magnani, P. Puliti, M. Stefanon, *Inst. Meth. A* 217 (1988) 611–616.
- [18] R. Coppola, R. Kampmann, M. Magnani, P. Staron, *Acta Mater* 46 (1998) 5447–5456.
- [19] R. Coppola, M. Klimenkov, R. Lindau, L. Porcar, M. Sepielli, M. Valli, D.J. McGillivray, J. Trehwella, E.P. Gilbert, T.L. Hanley, in: *Proceedings of the 15th International Small-Angle Scattering Conference*, 2012 ISBN 1 921268 15 8.
- [20] R. Coppola, M. Klimenkov, R. Lindau, B.R. Pauw, M. Valli, in: *Defect Distributions in Irradiated Nuclear Steels as Investigated with Complementary TEM and Small-Angle Neutron Scattering*, Oral Presentation at the EMMM 2013 Conference, Kyoto, November 2013.